Papers in the Earth and Atmospheric Sciences   Earth and Atmospheric Sciences, Department of

11-2015

8000 years of environmental evolution of barrier–lagoon systems emplaced in coastal embayments (NW Iberia)

Rita González-Villanueva
Universidade de Vigo, Spain, ritagonzalez@uvigo.es

Marta Pérez-Arlucea
Universidade de Lisboa, Portugal

Susana Costas
University of the Algarve, Portugal

Roberto Bao
Universidade da Coruña, Spain, roberto.bao@udc.es

Xose L. Otero
Universidade de Santiago de Compostela, Spain

See next page for additional authors

Follow this and additional works at: http://digitalcommons.unl.edu/geosciencefacpub

Part of the Geomorphology Commons, Hydrology Commons, Oceanography Commons, Other Environmental Sciences Commons, Paleobiology Commons, and the Sedimentology Commons

Authors

Rita González-Villanueva, Marta Pérez-Arlucea, Susana Costas, Roberto Bao, Xose L. Otero, and Ronald J. Goble

8000 years of environmental evolution of barrier–lagoon systems emplaced in coastal embayments (NW Iberia)

Rita González-Villanueva,[1,2] Marta Pérez-Arlucea,[2] Susana Costas,[3] Roberto Bao,[4] Xose L. Otero,[5] and Ronald Goble[6]

1 Departamento de Xeociencias Mariñas e O.T. (XM1), Universidade de Vigo, Spain
2 Coast, Water and Surface Processes Research Group, Instituto Dom Luiz, Universidade de Lisboa, Portugal
3 Centre for Marine and Environmental Research (CIMA), University of the Algarve, Campus de Gambelas, Portugal
4 Centro de Investigacións Científicas Avanzadas (CICA), Facultade de Ciencias, Universidade da Coruña, Campus de A Coruña, Spain
5 Departamento de Edafoloxía e Química Agrícola, Facultade de Bioloxía, Universidade de Santiago de Compostela, Spain
6 Department of Earth and Atmospheric Sciences, University of Nebraska–Lincoln, USA

Corresponding author: Rita González-Villanueva, Departamento de Xeociencias Mariñas e O.T. (XM1), Universidade de Vigo, 36310 Vigo, Spain; email ritagonzalez@uvigo.es

Abstract

The rocky and indented coast of NW Iberia is characterized by the presence of highly valuable and vulnerable, small and shallow barrier–lagoon systems structurally controlled. The case study was selected to analyse barrier–lagoon evolution based on detailed sedimentary architecture, chronology, geochemical and biological proxies. The main objective is to test the hypothesis of structural control and the significance at regional scale of any highenergy event recorded. This work is also aimed at identifying general patterns and conceptualizing the formation and evolution of this type of coastal systems. The results allowed us to establish a conceptual model of Holocene evolution that applies to rock-bounded barrier–lagoon systems. The initial stage (early Holocene) is characterized by freshwater peat sedimentation and ended by marine flooding. The timing of the marine flooding depends on the relation between the elevation of the basin and the relative mean sea-level position; the lower the topography, the earlier the marine inundation. Thus, the age of basin inundation ranged from 8 to 4 ka BP supporting significant structural differences. Once marine inundation occurred, all systems followed similar evolutionary patterns characterized by a phase of landward barrier migration and aeolian sedimentation towards the back-barrier (i.e. retrogradation) that extended circa 3.5 ka BP. The later phases of evolution are characterized by a general trend to the stabilization of the barriers and the infilling of the lagoons. This stabilization may be temporally interrupted by episodes of enhanced storminess or sediment scarcity. In this regard, washover deposits identified within the sedimentary architecture of the case study explored here suggest pervasive high-energy events coeval with some of the cooling events identified in the North Atlantic during the mid- to late Holocene.

Keywords: barrier–lagoon, geochemistry, overwash, rocky coast, sedimentary environments, sedimentology

Introduction

The recent evolution of coastal sedimentary areas resulted from eustatic sea-level rise after the Last Glacial Maximum (LGM). Sea-level was located 110–130 m below the present level during the LGM and experienced a rapid rise from 19 to 7 cal. ka BP (Cameron et al., 1987; Clark et al., 2004, 2009; Dellwig et al., 1999). The sea-level curves for the NW Iberia indicate that sea-level was about 7–5 m (Alonso and Pages, 2010) and 5 m (Leorri et al., 2012a, 2012b) below present mean sea-level (MSL) at the beginning of the highstand (circa 7 cal. ka BP). Following the highstand, sea-level continued rising but at a lower rate. Sea-level deceleration during the late Holocene has been repeatedly invoked as the trigger of sand barrier initiation (Clemmensen et al., 1996; Niedoroda et al., 1985; Otvos, 1981; Psuty et al., 2000; Rampino and Sanders, 1981). Sediments stored in the shoreface migrated inland with sea-level rise, forming

barriers and isolating wetlands from the open sea (Bao et al., 2007; Cearreta et al., 2003; Freitas et al., 2003).

Coastal lagoons can form and develop simultaneously or after barrier attachment, although their existence is genetically linked to sand barriers (Cabral et al., 2006; Costas et al., 2009; Demarest and Leatherman, 1985; Nichols, 1989). Local aspects such as the nature of the basement, coastal orientation, topography, physiography, sediment source and so on induce differences in the coastal systems' evolution (Costas et al., 2009). These local aspects are prominent in the NW Iberian coast, which is rugged and cut by incised river valleys (*rias*). This rocky characteristic favours the development of several boulder beaches along this coast (Blanco- Chao et al., 2002; Feal-Perez et al., 2014). The barrier–lagoon systems are located within small and highly indented bays in the *Rias*. Lagoons located in these embayments are relatively shallow and <1 km² in area. These en-
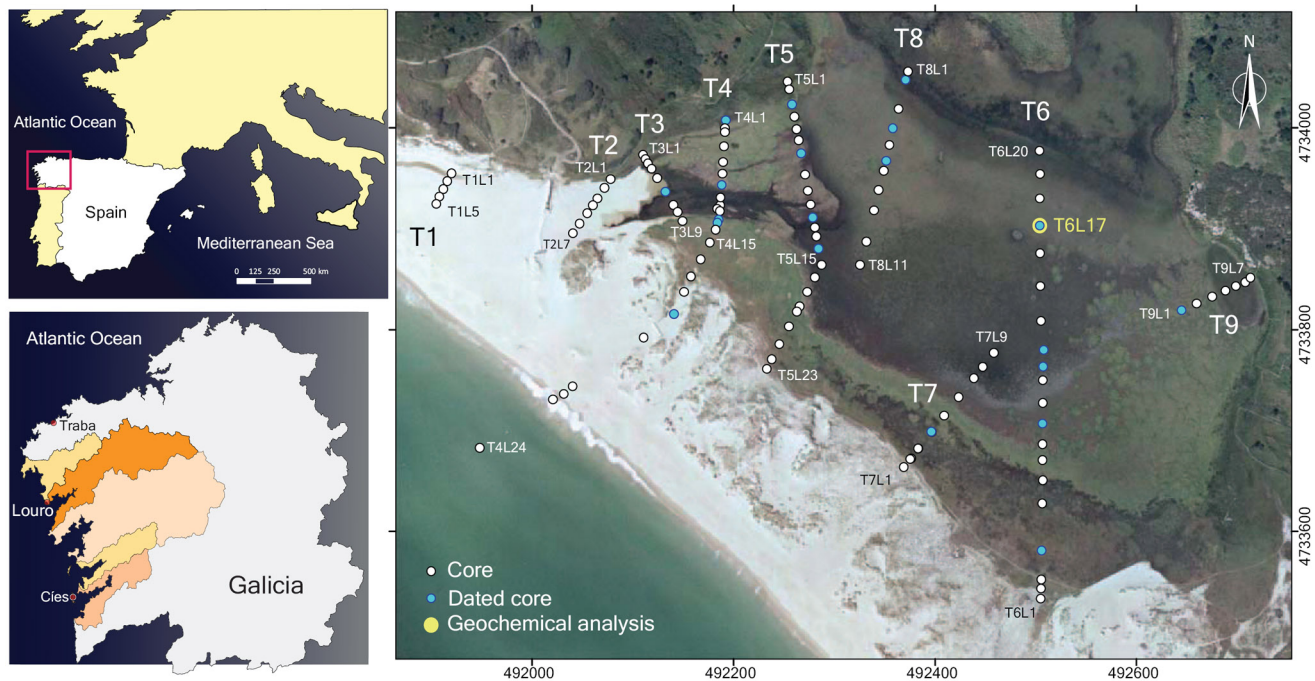
Figure 1. Location of the study site (Louro) at the North Slope of the Ría de Muros-Noia. The colour areas in the map of Galicia represent the catchments of the Rías Baixas. Right side: aerial photograph of Louro barrier–lagoon (2003), showing the position of the studied cores, the dated cores and the core selected for geochemical analysis (i.e. core T6L17).

vironments constitute one of the most singular geomorphological elements in the NW Iberian Peninsula with a special ecological, economic, landscape significance and are protected by the Habitat Directive of European Union (Directive 92/43 of 21 May 1992 on the conservation of natural habitats and of wild fauna and flora). Indeed, most of them are natural habitats of different protected taxa, some of them listed in the Galician Catalogue of Endangered Species, playing an important role in their preservation.

During the last 1000 years, coastal evolution has been interfered by human activities, which superimpose on the natural processes (Bao et al., 1999; Freitas et al., 2003; Munoz Sobrino et al., 2014). This resulted from the high pressure of population over coastal areas since prehistoric times, consuming and altering its natural resources (European Environmental Agency (EEA), 2006). Coastal systems have therefore been threatened, deteriorated or destroyed by changes in the land use or in the inputs of freshwater and sediment transport from catchments.

Previous works dealing with the Holocene evolution of barrier–lagoon systems in the NW Iberian coast (Bao et al., 2007; Costas et al., 2009; Devoy et al., 1996) highlighted the role of the topographic inheritance in the earlier evolution of these systems. However, two major questions regarding the late Holocene evolution of these coastal systems along the rocky Atlantic Galician coast remain unanswered: (1) Is there a common pattern in the evolution of these structurally controlled systems? (2) Could the sedimentary archive of these systems be used as an indicator of climatic or environmental regional changes? These are key questions that need an answer in order to understand the evolution of these systems, on a solid chronostratigraphic framework, to evaluate the role played by natural factors in their environmental evolution and to analyse their current situation regarding the impact of recent human activities.

In the present work, the Holocene evolution of a barrier– lagoon system is investigated in relation to the processes and factors involved in its formation. Due to its well-preserved state, the study area (Louro lagoon) clearly represents a suitable case to increase our understanding of the Holocene evolutionary patterns and processes involved. The main objectives of this work are twofold: (1) to

establish a Holocene evolutionary pattern of barrier–lagoon systems in rock-bounded embayment along NW Iberia and (2) test the significance of these sedimentary records as climatic change indicators at a regional scale. The comparison with other similar systems in the Atlantic Iberian coast allows the identification of regional signals versus local responses.

Study area

The coastal landscape in the Galician Atlantic Margin is highly dominated by Hercynian granite cliffs between the *Ria* systems. Coastal sand barriers are located in small embayments in the external areas of the *Rias*. Quaternary deposits of alluvial or coastal environments cover the substrate in some areas (Casquet and Fernandez de la Cruz, 1981). Louro barrier–lagoon coastal system (42°45′23″N, 9°5′36″W; Figure 1) is one of the best-preserved wetland environments in Galicia and is catalogued as a Site of Community Importance (Natura 2000 Network, Directive 92/43/EEC) under the Habitats Directive of the European Union. The sedimentary complex consists of an attached barrier, enclosing a brackish lagoon. The lagoonal surface varies seasonally between 0.042 and 0.25 km^2, as a function of rainfall and fluvial input. The lagoon is shallow despite strong water-level fluctuations (Perez-Arlucea et al., 2011), which impose important changes in salinity (Cobelo-Garcia et al., 2012). During the closed stages of the lagoon, there is an impoverishment of the chemical and microbiological quality of the water (Fraga, 2013). The freewater surface reduces substantially during the summer (almost dry), being confined to a small area in the northeast, where the lagoon is almost permanent. In this area, the water depth reaches 2 m during high water levels, whereas shallower parts are around 0.5 m deep. The catchment areas of the small rivers entering the lagoon are about 3.5 km^2. The watershed is 300 m high maximum, and the hydrographic network is mostly composed of small ephemeral rivers and creeks. The main river is only 10 km long, with a marked seasonal discharge. In the summer, the river is almost dry, affecting the water level in the lagoon. Bedload material is very poorly selected and contains practically no sand.

As mentioned in the "Introduction" section, in this work a comparison is made between the study area (Louro) and other similar systems in the same region: Traba and Cies.

Traba barrier–lagoon system is located at the north of the study area (Figure 1). The sand barrier is about 2.5 km long and has an average width of 400 m, with an NE-SW orientation. The sand barrier comprises a beach and a dune-field dominated by low-rise dunes interrupted by few storm corridors (Devoy et al., 1996). Traba coastal wetland is at present a shallow water body with a maximum depth of 1.5–2 m, which has marine influence only during storm events (Bao et al., 2007).

The Cies barrier–lagoon system is located to the south of the study area (Figure 1). The system consists of a natural 1 km long barrier that confines a shallow and saline lagoon. The barrier is oriented north to south, and two rocky headlands constitute the terminations of the barrier to which it appears anchored (Costas et al., 2009).

Climatic conditions for the Rias Baixas area (southern Galicia) are oceanic with Mediterranean influence. The average temperature in Louro ranges between 10°C and 12°C in winter and 18°C and 20°C in summer. Precipitation values average 1100 mm yr^{-1} (Martinez Cortizas and Perez Alberti, 1999). The system is classified as meso-tidal following the terminology of Davies (1964), with an average tidal range of around 3 m. Following the Spanish recommendation for Maritime Works (Fomento, 1991), the wave directions to consider, accounting for the orientation of the coast, are those between the SSW and NNW. The swell direction is mainly from the NW, the wind sea is from the N and the SW waves are frequently associated with storms. In the Louro barrier–lagoon system, these waves are responsible for morphological changes observed in the beach and for promoting the breaching of the barrier (Almecija et al., 2009).

Materials and methods

Geomorphological mapping, stratigraphy, geochemical, textural and diatom analyses were conducted in Louro aiming at exploring the regional and local driving signatures during the Holocene evolution. In addition, we attempted to establish the anthropogenic imprint in recent times in the context of the dynamic processes operating in the sedimentary system.

Geomorphological setting

The characterization of existing environments in Louro derives from field observations during coring campaigns, combined with the recent aerial photographs and Laser Imaging Detection and Ranging (LiDAR) Digital Terrain Models (DTMs).

DTMs were obtained with a high-resolution Terrestrial Laser Scanner (Class-1 TSL-RIEGL model LMS Z-390i) in 2009. Additional airborne LiDAR datasets were surveyed in 2010 (Grant from IGN; Spanish National Geographic Institute). LiDAR data were collected in ellipsoidal heights that were later transformed to orthometric heights, referred to the AMSL (Alicante Mean Sea-Level – Spanish Datum System). The AMSL reference is 2.328 m above the MSL; see www.puertos.es for more information. The maps were based on the Geodetic Reference System ED50 (UTM zone 29N). All collected data were geo-referenced and the digital data were compared with the aerial photographs to study the modern environments within the lagoonal complex and establish the detailed cartography of the geomorphological units.

Facies analysis

The study of the sedimentary architecture and the evolution was based on more than 100 cores (Gonzalez-Villanueva, 2013), with a penetration depth up to 5 m, obtained with a TESS-1 suction corer (Mendez et al., 2003). All cores were geo-referenced to a UTM coordinate system (ED50) with an RTK-GPS, and the elevations were taken with respect to the AMSL. The cores were macroscopically described and sampled for laboratory analysis. All cores were corrected for compaction during coring, considering penetration depths.

A detailed logging of all the cores was carried out once the cores were longitudinally split and opened. Different facies and associations were visually separated based on lithology, fossil and organic contents, colour, sedimentary structures and textural characteristics (grain size, sorting, etc.). The latter were confirmed and more accurately represented based on textural and compositional analysis. For those, the cores were sampled every 5 cm. Grain size measurements of the <1 mm fraction were made with an LS100 Coulter Counter. Fraction >1 mm was measured by sieving. Results from both methods were integrated and the statistical analyses of the data were performed using Gradistat software (Blott and Pye, 2001). These analyses were performed at the University of Barcelona. Diatom and geochemical analyses were performed in some cores, described in the following subsections, for a better differentiation of the visually identified facies.

Topographic profiles were surveyed using an RTK-GPS system to construct 2D correlation profiles with the cores and establish the facies architecture (Figure 1). Comparison with the sediment characterics in modern sedimentary environments allowed recognition of the different facies and the reconstruction of their geometry.

Palaeoecological proxies: Diatom analysis. Due to their narrow tolerance to environmental conditions and their ubiquity in all coastal wetlands (Trobajo and Sullivan, 2010), diatom remains were used for a better facies characterization and palaeoecological reconstruction of the lagoon. For this, sediment samples (0.1 g of dry weight) belonging to each sedimentary facies represented in core T6L17 were processed according to standard techniques (Renberg, 1990). Cores T4L2, T8L9 and T10L1 were also checked for diatom content, but due to their lower valve concentration, and/or worse preservation than in core T6L17, they were disregarded for any further study. The cleaned subsamples of core T6L17 were dried onto coverslips and mounted onto microscope slides with Naphrax (RI = 1.74). Identifications were performed at a magnification of 1000× with a Nikon Eclipse 600 microscope with Nomarski differential interference contrast optics. Due to the low diatom content in the samples, and since most of the valves showed a high degree of corrosion and/or fragmentation, abundances of the main taxa making up the assemblages were estimated on a semi-quantitative basis (Sancetta, 1979). Diatom-based reconstruction of sedimentary environments was based on the methodology of Vos and Wolf (1993).

Geochemical characterization. Core T6L17 (Figure 1) was selected due to its central position for a better differentiation of lagoonal facies. The core was sampled for geochemical analyses every 20–50 mm. Percentages of sand and silt + clay fraction contents were determined (Gee and Bauder, 1986). Total carbon (TC) and total nitrogen (TN) were analysed with a TruSpec CHN, and the total sulphur (TS) with a Leco CS-144 DR, over ground samples. Samples were heated at 450°C to measure total inorganic carbon (TIC) (Cambardella et al., 2000). Total organic carbon (TOC) content was estimated by subtracting the TIC from the TC.

Total concentrations of Fe, Mn, Al, P and trace elements were measured from 1 g of dry and ground sample of sediment. Total Fe (TFe), Al (TAl), Mn (TMn) and P (TP) and trace metals were extracted by adding 15 mL of a mixture of HNO_3:NCl:HF (9:3:3, v/v/v) in a 120-mL Teflon bomb containing 0.5 g of sample, previously lyophilized and ground, and heating the mixture in an Ethos Plus (Milestone) microwave for 20 min. The metal concentration was measured in a Perkin Elmer Optima 4300DV ICPMS spectrometer.
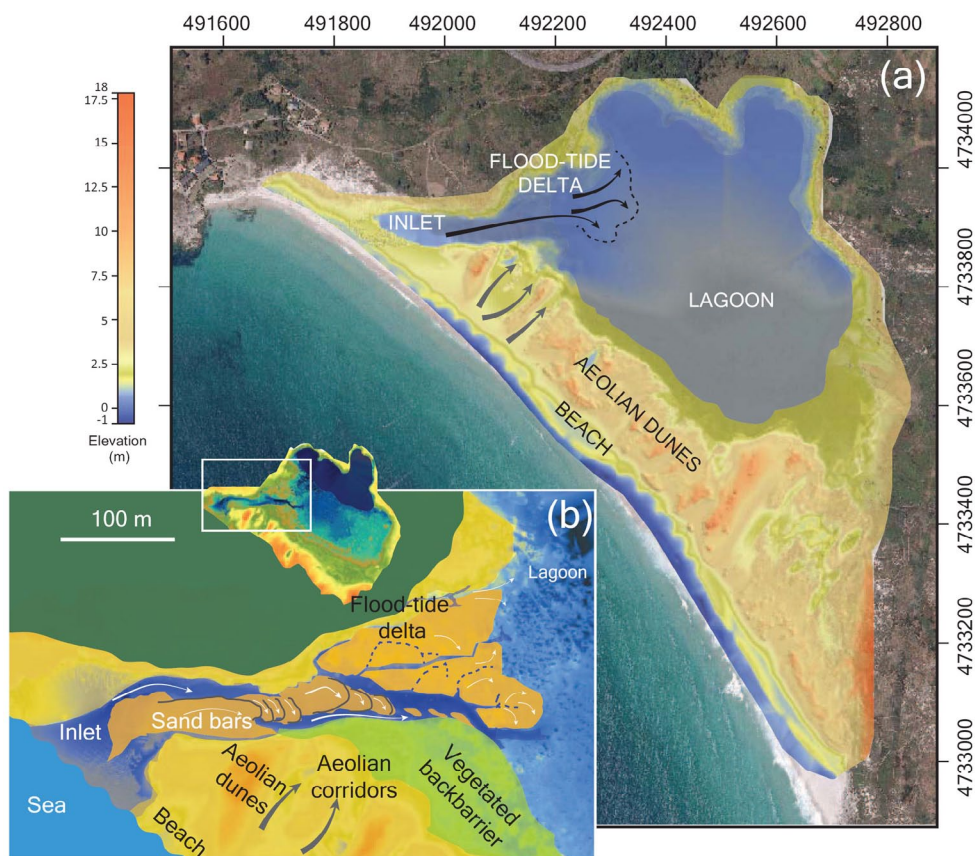
Figure 2. (a) Morphosedimentary units in Louro barrier–lagoon system over the aerial photo and overimposed LiDAR image. (b) Detail of the flood-tide delta and the inlet area. The present-day active distributary channel is the one located south of the delta, which transports sand towards the lagoon when the inlet opens.

Chronostratigraphy

Chronostratigraphy was based on both OSL (optically stimulated luminescence) and ^{14}C AMS (accelerator mass spectrometry) dates. A total of 20 OSL samples from five cores were collected using double coring with the same exact length; one of the cores was used for logging and identifying the layers to date and the second for dating at the selected depth. The samples were analysed at the Geochronology Lab of the Department of Earth and Atmospheric Sciences (University of Nebraska–Lincoln, USA). Quartz and feldspar grains were extracted by flotation using a 2.7 g cm^{-3} sodium polytungstate solution, then treated for 75 min in 48% HF, followed by 30 min in 47% HCl. The sample was then re-sieved and the <90 μm fraction discarded to remove residual feldspar grains. The etched quartz grains are mounted on the innermost 2 mm of 1 cm aluminium discs using Silkospray. Chemical analyses were carried out using a high-resolution spectrometer. Doserates were calculated using the method of Aitken (1998) and Adamiec and Aitken (1998). The cosmic contribution to the dose-rate was determined using the techniques of Prescott and Hutton (1994). OSL analyses were processed with a Riso Automated OSL Dating System Model TL/OSL-DA-15B/C. AMS radiocarbon analyses were performed in 31 samples from 17 cores using in situ bivalve shells (entire and articulated) and organic-rich sediments, at the Center for Applied Isotope Studies (University of Georgia, USA). Calibration of radiocarbon dates was conducted using IntCal09 (Reimer et al., 2009) for peat and organic mud while Marine 04 (Reimer et al., 2009) was applied to bivalve shells, by means of Calib 6.1.0 software (Stuiver et al., 2005). Two sigma (2σ) age ranges (95.4% probability) were considered (Bjorck and Wohlfarth, 2001).

Results

Geomorphological setting

The Louro barrier–lagoon system is formed by an attached barrier with an intermittent inlet and a shallow lagoon (Figure 2). The barrier comprises an exposed beach (Area Mayor Beach) backed by a semi-vegetated dune complex with maximum elevations of 15 m. The beach has an NW-SE orientation, being highly exposed to the SW winds and storm waves. Almecija et al. (2009) developed a detailed study of beach morphodynamics, and classified it as an intermediate morphotype following the beach classification proposed by Masselink and Short (1993), evolving towards a more dissipative morphology during high-energy events associated with SW winds. The dune complex is crossed by a series of aeolian corridors. The topographic elevation is nowadays too high (>4 m) to experience overwash, even during the most intense storms, which happen during the autumn and winter seasons (Perez-Arlucea et al., 2011).

The identified sedimentary environments comprise several deposits. Apart from the aforementioned beach–dune complex, a set of coalescing, abandoned washover fans appear in the proximal back-barrier area, attached to the dune-field. The washover fans are nowadays covered by aeolian sands and mud, and colonized by a vegetation cover typical of high saltmarshes. In the north end of the coastal barrier, a flood-tidal delta was developed related to an ephemeral inlet (Figure 2). Most of the delta is abandoned and covered by saltmarsh plants. However, when the inlet breaches the barrier a channel is active in the southern margin of the tidal delta (see Figure 2b).

The barrier is composed of well-sorted, white and medium sand mixed with carbonate grains of bioclastic origin. Aeolian sand is better sorted and more mature compositionally, with higher pro-

Table 1. Sedimentary facies identified in the record of Louro barrier–lagoon.

Facies associations	Code	Lithology and texture	Sedimentary structure, shells and organics	Diatom content (dominant taxa)	Environment
Sand barrier	Fc1	Variable sorting, white and yellow, mixed siliciclastic-carbonate coarse to fine sands (quartz, micas and feldspars)	Echinoderm fragments Open marine bivalve and gastropods fragments	Barren	Beach
	Fc2	Very well sorted and rounded, white, medium sand (quartz)	Parallel lamination, ripples, grain flow units, millimetre-scale heavy mineral accumulation layers	Barren	Dune
	Fc3	Poorly sorted, sandy sediments and some carbonate grains	Shell lags and broken shells. Rip-up clasts and pebbles	Barren	Tidal inlet
Flood-tide delta	Fc4	Poorly sorted, sandy to muddy sediments and carbonates	Massive, shell lags, rip-up clasts and coarse mineral grains	Barren	Delta channels
	Fc5	Poorly sorted, mixed siliciclastics and carbonates. Medium to fine sand	Shell fragments from the outer (beach and rocky shore)	Barren	Sandy delta, delta lobes
	Fc6	Fairly well-sorted alternations of fine to very fine-grained sand and mud	Massive	Barren	Muddy delta and inter-channel
Washover	Fc7	Poorly sorted, brownish, pebbly sand and coarse shell fragments and pebbles. Siliciclastic sands and muddy sands	Transported shell fragments Finning upward sequences	Barren	Washover
Lagoon	Fc8	Poorly sorted, grey, medium to very fine mixed siliciclastic-carbonate grains in an organic matrix	Rooting and bioturbation Whole shells and shell fragments of bivalve and gastropods	*Opephora mutabilis, Ctenophora pulchella, Cocconeis placentula* and *Cocconeis peltoides*	Sandy lagoon. Water-level oscillation
	Fc9	Poorly sorted, brown and grey, very fine. Mixed siliciclastic-carbonate grains and mud	Massive and high organic matter content Whole and broken shells of bivalves and gastropods	*Cocconeis placentula, Opephora mutabilis* and *Staurosira construens* aff. *venter*	Muddy lagoon. Permanent flooding
Marginal deposits	Fc10	Peat Poorly sorted, brown, fine to medium sands (quartz) and mud	Massive and high organic matter content Plant remains, seeds and wood fragments	*Cocconeis placentula* and *Diatoma tenuis*	Marginal lagoon

portions of very well-rounded and well-sorted quartz grains. Sediment in the lagoon is very variable in composition and grain size. Sediments in the area of the lagoon closer to the barrier are sandier than in the deeper and inner areas of the lagoon, which show an increase in the content of organic-rich mud. The contact between both types of environments is sharp, although it is possible to observe some areas of gradual transition.

Facies analysis

Facies associations and architecture are described for the Holocene record based on the analysis of all core logs and sampling. A total of 10 sedimentary facies are identified considering sediment composition, texture, fauna/floral content and geometry. The facies architecture is based on nine core transects (Figure 1), although only the most representative four are presented here. A brief summary of the Holocene facies cored in the subsurface of the Louro system is presented in Table 1. The 10 identified facies are grouped into five associations: sand barrier (Fc1–Fc3), flood-tide delta (Fc4–Fc6), washover (Fc7), lagoon (Fc8–Fc9) and marginal deposits (Fc10).

Sand barrier. It consists of facies Fc1, Fc2 and Fc3 (Table 1). This is the dominant facies association in the depositional record of Louro. Fc1 is interpreted as beach sediments based on its heterogeneity and roundness, which are similar to the analogues of the present beach. Fc2 represents aeolian sediments based on its composition (largely dominated by quartz), high textural maturity (very well sorted and rounded to well-rounded grains) and modern counterparts. Fc3 cor-

respond to the tidal inlet infill, which is very recent considering that each time the inlet opens, the flow excavates up to 2 m deep channel (Perez-Arlucea et al., 2011). The lateral area of inlet migration is very restricted due to the confinement forced by local rock outcrops in the north and the sand dunes at the south.

Flood-tide delta. Facies Fc4, Fc5 and Fc6 constitute the flood-tide delta deposits. Differences within this association are a consequence of the proximal or distal position of the deposits relative to the delta. As a result, three major facies, representing different depositional environments within the flood-delta, have been identified: (1) distributary channels (Fc4), consisting of coarse sands and shell lags, with frequent rip-up clasts and pebbles; (2) sandy delta and delta-lobe facies (Fc5) that consist of fine and medium sand in the proximal area; and (3) muddy delta facies (Fc6), which are characterized by high organic matter content and are located in the distal area (Table 1).

Washover fan. It is represented by facies Fc7 (Table 1). This is characterized by shell fragments derived from the benthic communities living in the shoreface of the adjacent beach and coarse sediments from the barrier (mainly beach sediments) transported into the lagoon by sporadic marine flooding during high-energy storm events. In turn, this process re-suspends muddy sediments within the lagoon, which settle once high-energy events end.

Lagoon. It comprises two facies: Fc8 and Fc9. The sediment in the lagoon derives from two major sources. One part is wind-blown sand

sourced by the coastal barrier (Fc8, sandy lagoon), while the other part consists of muddy particles transported by rivers and soil erosion by runoff (Fc9, muddy lagoon). The TOC (Figure 3b) is very low in lagoon facies (<0.5%). Eventually, Fc9 and some sandy levels may have higher values due to the presence of rip-up clasts enriched in organic carbon (1.2– 2.7%). TN shows similar trends to TOC and an excellent correlation ($rs = 0.734$, $p < 0.001$, $n = 68$; Supplementary Table 1, available online), suggesting that TN content is explained by organic matter enrichment. The molar relation TOC/TN (Figure 3c) shows similar values to those of marine organic matter, alternating with values corresponding to continental vascular plant organics (TOC/TN > 20), corroborating the two major sources of sediment to the lagoon suggested by the mineralogenic component of the sediment.

In both facies, concentrations of total Al and Fe are very low (2% and 1%, respectively) (Figure 3d). Both elements, which have a good correlation with organic carbon and mud content, have a similar behaviour (Supplementary Table 1, available online). TP (<300 mg kg^{-1}), TMn (<150 mg kg^{-1}) and total trace metals (in general <10 mg kg^{-1}) are very low too (Figure 3e and f), compared with other sedimentary environments with a granite sediment source (Macias Vazquez and Calvo de Anta, 2009; Merian, 1991).

The observed low concentration of macro and trace elements is probably due to the dilution effect of the sand (mainly quartz sands), which maintained a negative correlation (Supplementary Table 1, available online). Nevertheless, there is a significant increment of all these elements related to the organic-rich muddy zones. TFe, TAl and TOC show a highly positive correlation, along with TP, TMn and total trace metals, indicating a strong association between these elements and the organic matter, clay content and Fe/Mn oxides and hydroxides (Supplementary Table 1, available online). These high positive correlations indicate that these trace elements have a natural source, which agrees with the fact that once the normalization with Al is done, most part of the maximum values disappear (Figure 3f).

Facies Fc8 represents the lagoon with important water oscillations where aeolian sand eventually accumulates. This facies showed levels almost barren of diatoms. Whole valves were rare but, as expected, an epipsammic diatom, *Opephora mutabilis* is the most frequent taxon. *Ctenophora pulchella, Cocconeis placentula* and *Cocconeis peltoides* are subdominant. Fragments of *Diploneis* spp., unidentifiable at the species level, were also recorded. Values of TS (Figure 3b) are extremely low (<0.1%). A sub-facies Fc8b has been defined in terms of increased mud and bioturbation (Figure 3), including rooting, manifested by a sharp change in colour. The diatom content in this facies transition shows at the base the highest abundances of marine/brackish epipsammic diatoms, made up not only by *O. mutabilis* but also by *Planothidium delicatulum*. By contrast, the top is dominated by the freshwater tychoplanktonic *Staurosira construens* aff. *venter*, with *O. mutabilis* and *P. delicatulum* as a minor component of the assemblage.

The facies Fc9 corresponds to the permanently flooded lagoon dominated by muddy sedimentation. Diatom assemblages are dominated by the freshwater epiphytic *C. placentula*, whereas the marine/brackish epipsammic *O. mutabilis* and brackish/freshwater *S. construens* aff. *venter* act as subdominant species. The marine/brackish epiphytic *C. pulchella* and *Synedra tabulata* also appear in low numbers. The TS reaches higher values than in Fc8, close to 1%. The high correlation between TS and TOC, and the lack of relation with Fe, is highly significant, indicating an organic origin for S (Supplementary Table 1, available online).

Marginal deposits. Facies Fc10 represents shallow peripheral areas saltmarsh. Fc10 is composed of organic-rich sediments and/ or muddy black peat derived from plant remains, seeds and wood fragments sometimes mixed with aeolian sand. Bioturbation by rooting is very common. Diatom assemblages in these facies are dominated by the freshwater epiphytic *C. placentula* and *Diatoma tenuis*. Relatively high values of TOC (>8%), reaching typical levels of peat materials, are characteristic of this facies, as well as higher values of TS (Figure 3).

Chronostratigraphy

The chronostratigraphy of Louro barrier–lagoon is based on 20 OSL samples (Table 2) and 31 ^{14}C samples (Table 3). Dates obtained from the two different dating techniques were consistent, as documented in the literature (Clemmensen et al., 2009; Gonzalez-Villanueva et al., 2011; Hou et al., 2012; Murray and Clemmensen, 2001). The results from both techniques have been integrated here using the notation AD/BC in Tables 2 and 3. 2D correlation panels were constructed to delineate the sediment architecture and reconstruct the evolutionary stages during the last 8000 years. The resultant OSL ages correspond to a time interval between 5.31 and 0.18 ka, within the middle and late Holocene Sub-epoch. The ^{14}C-dated samples cover a greater time interval which ranges from 8 to 1.2 cal. ka BP.

Facies architecture

Figure 4 represents the facies architecture based on core correlations. The sedimentary record overlays small drowned river valley carved into granite outcrops. Some of the collected cores reached the granite basement in the marginal areas of the lagoon, which is partially covered by a regolith. Peat layers overlying the basement, with a radiocarbon age circa 8 cal. ka BP constitute the oldest dated sediments. By contrast, the oldest dated barrier sediments yielded ages around 6 cal. ka BP (Figure 4).

Transect T6 (Figure 4) shows a transverse cross-section from the inner part of the barrier towards the lagoon with facies transitions from the barrier to the sandy lagoon and muddy lagoon deposits. These changes reflect the transition between the area of the lagoon directly influenced by the processes affecting the coastal barrier and the area of the lagoon dominated by the typical lagoon and muddy sedimentation. The sandy lagoonal facies show mixed faunal communities, sourced from the adjacent beach and lagoonal environments developed in the vicinity of the barrier. A flat surface, gently dipping landwards is observed today in the back-barrier covered with saltmarsh vegetation. This surface derives from the vertical accumulation of washover fans (T4 and T6, Figure 4). The washover facies (Fc7) shows typical wedgeshaped units, a few decimetres thick, thinning towards the lagoon and slightly dipping landwards. Their lateral distribution is not continuous. The internal structure is characterized by several vertically stacked, fining-upward sequences showing distinctive low-angle dipping sheets disrupting the sand barrier. There are some thin washover deposits in the deeper part of the section, with the oldest dating at 5.31 ka. During later depositional events (after 2.91 ka), washovers become thicker. The accumulation of muddy facies, interpreted as marginal deposits at the top of the washovers, supports a hypothesis suggesting prolonged periods of overwash inactivity.

Transect T3 is located at the north end of the barrier, where the beach is anchored to the basement and, in recent times, is sporadically affected by inlet breaching. Facies Fc1 (beach) and Fc2 (dune) lie on the rock basement at the landward side and are partially cut by the tidal inlet. Fc3 is representative of the latter. This facies presents a sharp and erosive contact between the base of the channel and the underlying strata. In the inlet area, the base cuts into the beach facies (Fc1). The tidal inlet observed in transect T3 occupies the position of the inlet observed in the aerial images since 1956 (Gonzalez-Villanueva, 2013). It has been suggested that the position of the channel depends on the beach topography during the
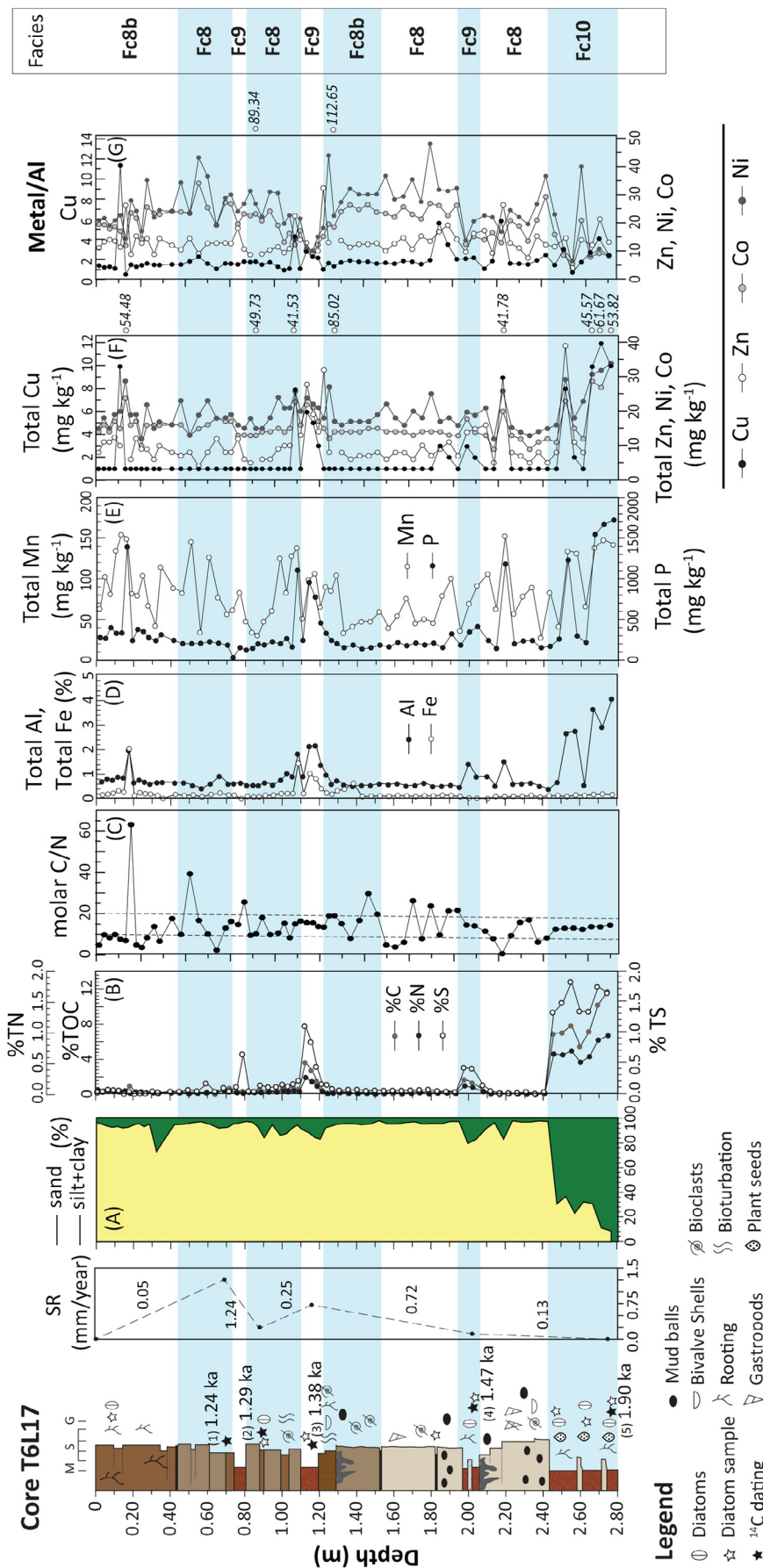
Figure 3. T6L17 core log, showing 14C AMS ages (cal. BP) and sedimentation rates (mm yr−1). A–C: vertical changes of different components in the sediments. The considered molar relation for non-vascular marine and vascular-terrestrial has been established between 8 and 20, respectively (Meyers and Lalliervergés, 1999). D–G: changes in the total concentrations of Al, Fe, Mn, P and trace elements and normalization of the metal concentration. Points outside graphs represent peak values. Identified facies using geochemical proxies are indicated at the right. Facies alternation is marked by horizontal blue bands.

Table 2. Luminescence dating results (OSL ages in years before (*) 2010; (–) 2008).

Sample	Depth (m, AMSL)	Laboratory ID	Cosmic (GY)	Dose-rate (Gy ka^{-1})	D_e (Gy)	No. of aliquots	Age (ka)	Cal. age (AD/BC)
T9L1a	1.48	UNL2590	0.19	1.69 ± 0.08	1.38 ± 0.07	51	(*)1.55 ± 0.12	AD 460
T9L1b	0.38	UNL2591	0.17	0.86 ± 0.05	2.09 ± 0.08	52	(*)2.42 ± 0.16	410 BC
T7L4a	2.04	UNL2107	0.19	0.94 ± 0.05	1.60 ± 0.05	48	(–)1.70 ± 0.11	AD 308
T7L4b	1.77	UNL2108	0.19	0.92 ± 0.05	1.70 ± 0.05	40	(–)1.85 ± 0.11	AD 158
T7L4c	1.06	UNL2109	0.17	0.93 ± 0.05	2.30 ± 0.06	42	(–)2.47 ± 0.15	462 BC
T6L4a	2.17	UNL2113	0.19	0.95 ± 0.05	1.77 ± 0.06	44	(–)1.86 ± 0.12	AD 148
T6L4b	1.17	UNL2114	0.17	1.06 ± 0.05	3.08 ± 0.08	42	(–)2.91 ± 0.17	902 BC
T6L4c	0.48	UNL2115	0.15	1.03 ± 0.05	3.90 ± 0.11	45	(–)3.80 ± 0.23	1792 BC
T6L4d	−0.31	UNL2116	0.14	0.95 ± 0.04	5.06 ± 0.14	48	(–)5.31 ± 0.33	3302 BC
T4L12a	2.03	UNL2043	0.19	0.92 ± 0.05	0.16 ± 0.01	40	(–)0.18 ± 0.02	AD 1828
T4L12b	1.95	UNL2044	0.18	0.98 ± 0.05	0.32 ± 0.02	40	(–)0.33 ± 0.03	AD 1678
T4L12c	1.13	UNL2045	0.16	0.99 ± 0.05	0.60 ± 0.01	63	(–)0.61 ± 0.03	AD 1398
T4L12d	0.88	UNL2046	0.15	0.90 ± 0.04	2.06 ± 0.01	41	(–)2.28 ± 0.13	272 BC
T4L12e	0.80	UNL2047	0.15	0.91 ± 0.04	2.52 ± 0.02	41	(–)2.76 ± 0.15	752 BC
T4L12f	−0.35	UNL2048	0.15	0.94 ± 0.04	4.13 ± 0.11	39	(–)4.38 ± 0.26	2372 BC
T4L18g	2.05	UNL2593	0.19	0.95 ± 0.05	0.21 ± 0.03	53	(*)0.22 ± 0.03	AD 1790
T4L18h	1.94	UNL2594	0.18	1.32 ± 0.07	0.34 ± 0.04	52	(*)0.26 ± 0.03	AD 1750
T4L18i	1.72	UNL2595	0.18	1.09 ± 0.06	0.36 ± 0.01	54	(*)0.33 ± 0.02	AD 1680
T4L18j	1.50	UNL2596	0.17	0.98 ± 0.05	0.39 ± 0.01	52	(*)0.40 ± 0.03	AD 1610
T4L18k	1.39	UNL2597	0.17	1.14 ± 0.05	0.46 ± 0.03	52	(*)0.46 ± 0.04	AD 1550

OSL: optically stimulated luminescence; AMSL: Alicante Mean Sea-Level – Spanish Datum System.

Table 3. Radiocarbon ages obtained by AMS 14C dating of bulk organic sediments (organic-rich sediments and peat) and articulated valves (*).

Sample	Depth (m, AMSL)	Lab. ID.	Δ^{13}C, ‰	^{14}C age, ka BP	Cal age ranges (2σ)	Median probability (ka cal BP)	Cal. age (AD/BC)
T3L6	−1.15	3320	-26.6	7.17 ± 0.030	7.942–8.024	7.985	6035 BC
T4L1	0.10	2808	-25.5	4.85 ±0.040	5.576–5.657	5.596	3646 BC
T4L1	0.97	2807	-26.14	3.3 ± 0.040	3.445–3.635	3.527	1577 BC
T4L6	−0.45	2809	-26	4.83 ± 0.040	5.473–5.552	5.545	3595 BC
*T4L11	−1.50	2158	-1.9	5.47 ± 0.050	5.714–5.955	5.844	3894 BC
*T4L12	−1.22	2810	-1.99	5.46 ± 0.040	5.723–5.922	5.835	3885 BC
T5L3	1.62	3321	-26	2.21 ± 0.025	2.151–2.318	2.233	283 BC
T5L3	0.69	3322	-26.3	3.27 ± 0.025	3.443–3.566	3.499	1549 BC
*T5L7	−1.38	3323	0.4	4.58 ± 0.040	4.688–4.864	4.805	2855 BC
*T5L10	−1.18	3324	-1.8	4.46 ± 0.030	4.531–4.778	4.648	2698 BC
T5L10	−1.43	3325	-21.9	6.15 ± 0.030	6.959–7.159	7.064	5114 BC
*T5L15	−0.17	3326	-2.3	4.15 ± 0.030	4.106–4.348	4.221	2271 BC
*T5L15	−1.45	3327	-10.5	4.84 ± 0.030	5.026–5.266	5.147	3197 BC
*T6L9	−1.01	2811	0.22	4.41 ± 0.040	4.425–4.717	4.570	2620 BC
T6L12	0.48	2812	-21.7	3.06 ± 0.040	3.201–3.374	3.285	1335 BC
T6L13	−1.83	2813	-24.01	4.49 ± 0.050	5.026–5.307	5.153	3203 BC
T6L17	1.41	4520	-23.6	1.3 ± 0.035	1.174–1.294	1.240	710 AD
T6L17	0.73	4521	-24.1	1.37 ± 0.035	1.256–1.348	1.295	655 AD
T6L17	0.52	4522	-23.8	1.5 ± 0.030	1.312–1.417	1.380	570 AD
T6L17	−0.13	4523	-21.7	1.59 ± 0.035	1.400–1.548	1.470	480 AD
T6L17	−0.69	4525	-21.3	1.95 ± 0.045	1.812–2.001	1.901	490 AD
T8L2	−1.85	2161	-24.8	3.67 ± 0.040	3.888–4.094	4.033	2053 BC
T8L3	−2.68	2814	-22.43	2.27 ± 0.040	2.156–2.268	2.244	294 BC
T8L3	−1.84	4532	-21.3	2.04 ± 0.035	1.922–2.072	1.997	47 BC
T8L5	0.23	2815	-23.52	1.97 ± 0.041	1.856–1.998	1.921	29 AD
T9L1	1.67	4533	-22	1.24 ± 0.035	1.072–1.266	1.181	769 AD
T9L1	1.37	4534	-21.9	1.57 ± 0.035	1.385–1.535	1.464	486 AD
T9L1	0.88	4535	-21.3	2.31 ± 0.035	2.300–2.363	2.335	385 BC
T9L1	0.62	4536	-21.1	2.28 ± 0.035	2.299–2.351	2.303	353 BC
T9L1	0.26	4537	-21.5	2.54 ± 0.035	2.490–2.603	2.624	674 BC
T9L1	−0.26	4583	-20.5	2.83 ± 0.025	2.861–3.001	2.931	981 BC

AMS: accelerator mass spectrometry; AMSL: Alicante Mean Sea-Level – Spanish Datum System.
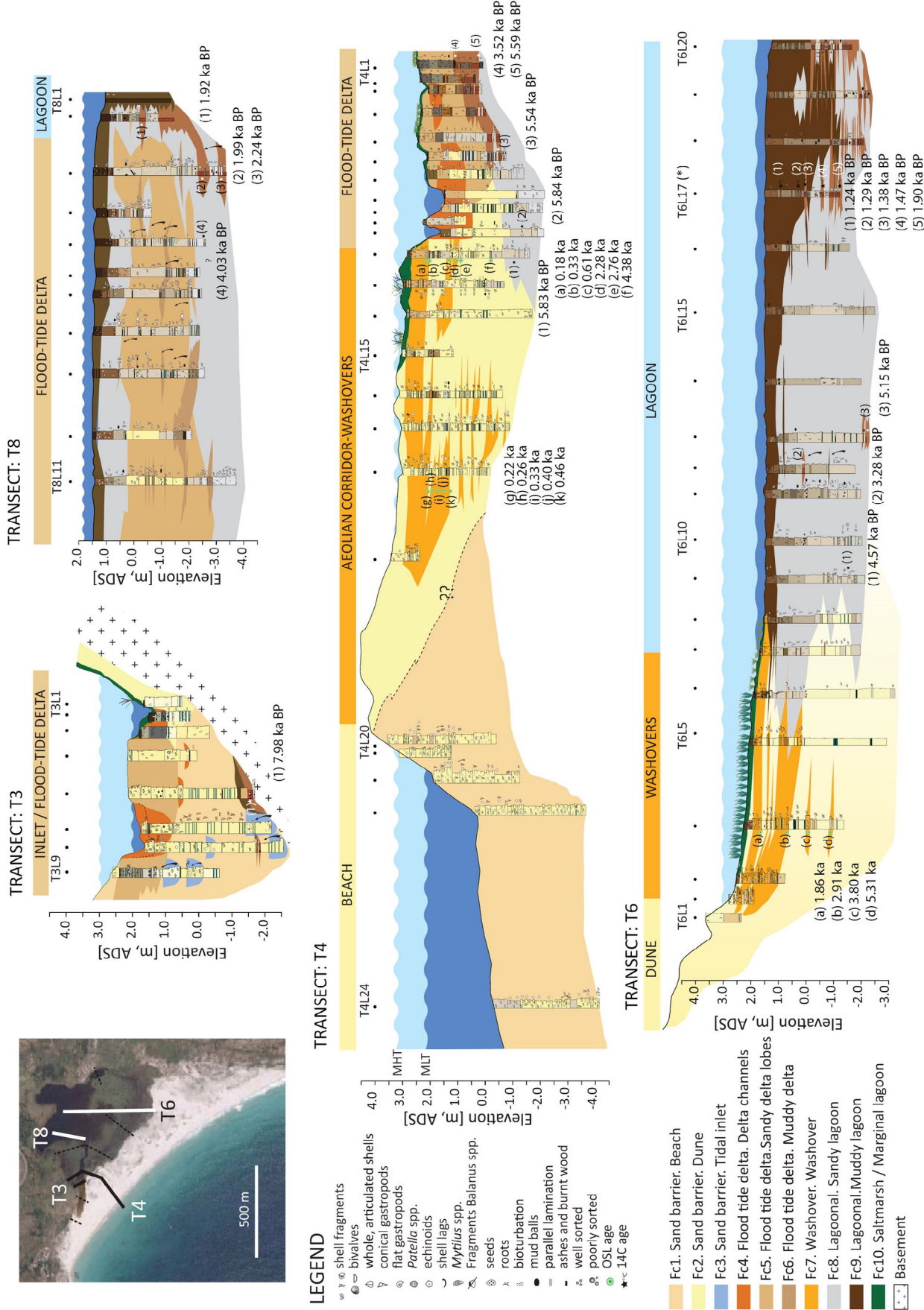
Figure 4. Selected core transects in Louro, showing facies associations and simplified architecture. A selection of AMS 14C ages is also shown. The map shows the position of the core transects selected for the figure.

breach of the barrier (Almecija et al., 2009; Perez- Arlucea et al., 2011). The channel bodies correspond to the inlet when the barrier breaches, showing a maximum depth of 2 m. The barrier and rocky outcrops at both extremes control the lateral extension of the channel. The latter was formed during the breaching events and generally opens just for a few days (Perez-Arlucea et al., 2011). Nowadays, water flow and sediments are transported along the main channel into the lagoon during the rising tides; this process is enhanced during storms and spring tides contributing to the development of the flood-tidal delta.

Transect T4 shows the spatial relation between the inlet, the flood-tidal delta and the barrier. This section was surveyed through one of the corridors avoiding the high crests within the dune-field. The most active distributary channel is located at this margin, close to the barrier. The delta is developed over sandy lagoonal facies at the centre and over muddy and marginal lagoon facies towards the north, along the inner and distal areas. The entrance of material through the open inlet forms flood-tide delta facies as the tide rises. When the inlet is closed, sediment inputs occur by overwash over the berm. Delta deposits exhibit complex and rapid changes showing channel switching, mouth bar progradation and inter-channel muddy areas (Transect T8, Figure 4), which are often removed by erosion, as indicated by the abundance of rip-up clasts. It is very difficult to separate individual sand lobes, as they are highly interconnected. However, it is possible to observe erosive contacts between the base of the channels and the underlying delta sediments. Sand lobe progradation and abandonment give way to fining-upward sequences in which an increase in mud and rooting is observed. A general increase in mud and vegetation (saltmarsh facies) can be observed in the most recent deposits of the delta due to a progressive decrease in the activity of the inlet and consequent delta abandonment in recent times. Channel fill deposits have a lenticular shape with erosive bases, most of which are covered by mud shell lags, ripup clasts and coarse mineral grains. The delta channels are represented by fining-upward sequences, including layers of mud and/ or marshy deposits at the top (Transect T8). Channel distribution, as observed in the aerial photos of the last decades, suggests that the number of active channels is limited since the flow usually concentrates in only one or two active channels (Gonzalez-Villanueva, 2013). It is therefore expected that the progressive abandonment of a channel will give way to discrete avulsion and delta-lobe switching.

A prominent feature in the lagoon and flood-tidal delta deposits is the existence of vertically stacked, m-scale, fining-upward units corresponding to the progradation of delta lobes and subsequent progressive abandonment (Transect T8). The shallow areas are composed of fine-grained grey sand with a variable content in organic matter. Towards the inner and deeper areas, the content in mud and organic matter increases, passing very abruptly into black, organic-rich mud, rich in clay. Vegetated areas, surrounding the lagoon, give way to peripheral marshes where peat develops. A general increase in mud is observed in the upper layers in the lagoon and delta area. Rooting by grasses and saltmarsh bulrush (*Scirpus maritimus*) and rushes (mainly, *Juncus maritimus*) is also common. These muddy deposits cover the antecedent washovers and the delta, supporting the hypothesis of progressive infilling and the reduction of the dynamism within the lagoon.

Interpretation and discussion

The internal architecture of the barrier–lagoon system supports the landward migration of the barrier parallel to the formation of a brackish lagoon in the back-barrier area in the early evolutionary stage. The following evolutionary stages involved a dynamic sedimentation regime including barrier accretion, inlet breaching,

flood-tide delta development and back-barrier overwash. Overwash processes were frequent in some stages of the evolution of the system, as reflected by the relative abundance of washover packages in some parts of the record. Considering the age and the spatial coverage of the washover fan deposits in the different sections, it is apparent that there has been a concentration of the overwash processes towards the north over time. The washover fans at the south end of the barrier are older, while at the north end they are relatively recent, suggesting an earlier abandonment of the storm corridors in the south. Nowadays, all the storm corridors have a relatively high elevation and are inactive. The youngest washovers and dune deposits dated within the system yielded an age around 0.2 ka. There is a gradual but rapid landward transition to the muddy lagoon facies (Figure 4). Facies distribution in the lagoon suggests the evolution towards conditions that are more confined, with sporadic opening of the inlet and reduced communication with the sea. A general increase in mud and organic matter is also apparent and indicates some degree of eutrophication, which could be recently enhanced by human activities in the catchment area (Fraga, 2013).

Anchoring and evolution of the barrier–lagoon system

The OSL and ^{14}C ages allowed the establishment of a well-constrained chronology for the onset and evolution of Louro barrier–lagoon complex in a timeframe. According to the architectural and age data (Figure 4; Tables 2 and 3), it was possible to identify four major phases in the barrier building and lagoon infilling processes. In addition, diatom and geochemical proxies allow differentiating episodes of environmental change in the inner lagoon (Figure 5), such as shifts in salinity, water depth and oxygen concentration.

Phase 1: 8–5.3 cal. ka BP (6050–3300 BC): Barrier onset. Phase 1 (Figure 5) is characterized by the initiation of the sedimentation within the lagoon, which is a consequence of the anchoring of the frontal barrier. The oldest ^{14}C age (7.98 cal. ka BP) corresponds to an anoxic peat layer, covering the basement, and suggests the marine flooding of the coastal basin with muddy deposits in marginal marshlands.

Sedimentation of sand in the back-barrier area commenced before 7.06 ka BP, as supported by the ^{14}C age of a marshland layer, overlying the sandy deposits. This suggests a frontal barrier allowing water retention in the back-barrier area and the organic-rich sedimentation. The elevation of the dated deposits suggests a MSL at least 3.5 m below the present MSL. Indeed, the deposition of peat layers in marginal areas at the north of the system between 5.84 and 5.54 cal. ka BP (Transect T4, Figure 4) reinforces the hypothesis of the establishment of a frontal barrier. The occurrence of aeolian sands within the organic-rich marginal deposits might be a consequence of sand inundation related to climate instability. Bao et al. (2007) inferred a lower MSL position (7 m below present MSL) circa 5.7 cal. ka BP from the interpretation of the sedimentary record of the Traba freshwater coastal wetland located to the north of Louro (Figure 1). Alternatively, Costas et al. (2009) inferred a position for MSL at least 4 m below present until 4 ka cal. BP in the Cies, located to the south of Louro (Figure 1). In both cases, authors relate the sedimentation within the explored coastal basins to the antecedent topography, which explains the high elevation of those systems relative to the present MSL and, subsequently, the differences observed in the timing of the marine flooding. This fact stresses not only the importance of coastal morphology to explain the asynchronous origin of the coastal wetlands in Galicia (or in other coastal embayment along the North Atlantic) but also that the application of littoral environments as sea-level indicators to reconstruct feasible sea-level curves must be done conscientiously (Alonso and Pages, 2010).
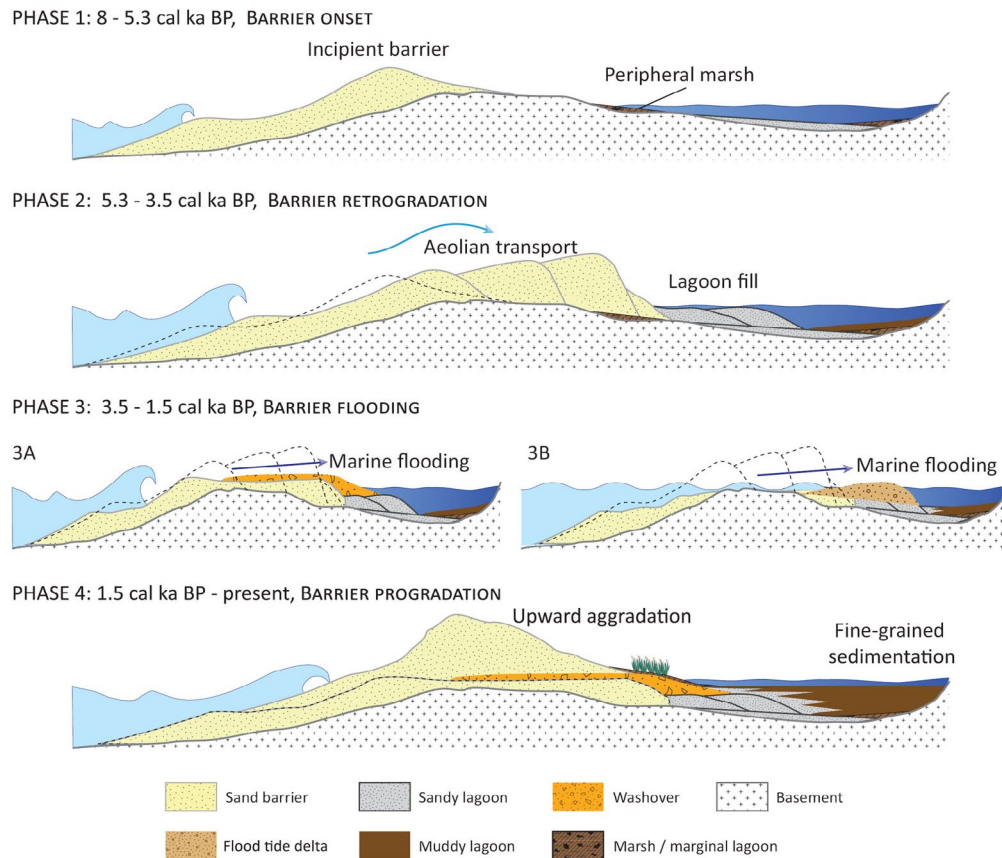
PHASE 1: 8 - 5.3 cal ka BP, BARRIER ONSET

Incipient barrier

Peripheral marsh

PHASE 2: 5.3 - 3.5 cal ka BP, BARRIER RETROGRADATION

Aeolian transport

Lagoon fill

PHASE 3: 3.5 - 1.5 cal ka BP, BARRIER FLOODING

3A

Marine flooding

3B

Marine flooding

PHASE 4: 1.5 cal ka BP - present, BARRIER PROGRADATION

Upward aggradation

Fine-grained
sedimentation

Sand barrier　　Sandy lagoon　　Washover　　Basement

Flood tide delta　　Muddy lagoon　　Marsh / marginal lagoon

Figure 5. Schematic illustration of the system evolution since 8 cal. ka BP. The dashed lines indicate the hypothesized sand barrier profile of each antecedent phase.

Phase 2: 5.3–3.5 cal. ka BP (3300–1550 BC): Barrier retrogradation. The lagoon infilling by aeolian sand characterizes Phase 2. This infilling is mostly due to barrier retrogradation. Radiocarbon ages from bivalves in life position dated between 4.80 and 4.22 cal. ka BP are indicative of marine influence in the lagoon allowing the growth of bivalve communities. This is corroborated by episodes of sporadic flooding supported by the occurrence of washover in Transects T6 and T4 dated between 5.31 and 3.80 cal. ka (Figure 4, Table 2), which imply a moderate permeability of the barrier at the end of this phase.

The first marine evidence in Cies lagoon was dated close to 3.7 cal. ka BP, suggesting barrier breaching and overwash (Costas et al., 2009). However, in the Traba freshwater coastal wetland, marine influence was never clearly recorded, probably as a consequence, again, of its high elevation and the distance to the shoreline (Bao et al., 2007). By contrast, the Traba sedimentary record documents an episode of aeolian sedimentation into the lagoon between 4 and 3.2 cal. ka BP (Bao et al., 2007; Devoy et al., 1996). Once again, the relation between the basin elevation and the MSL position can explain the delay of the marine influence in different coastal lagoons of the same regional area.

The mentioned features suggest that since the origin of the Louro coastal system circa 8 cal. ka BP, the sea-level was rising at a low rate, triggering the retrogradation of the system in a context of relatively low sediment availability. The latter explains the landward migration of the barrier through the formation of transgressive aeolian dunes and overwash deposits.

Phase 3: 3.5–1.5 cal. ka BP (1550 BC–AD 450): Barrier flooding. Marine flooding and barrier instability mark this phase (Figure 5). Washover deposits dated between 2.91 and 1.70 ka suggest extensive overwash of the central part of the sand barrier (Figures 3a and 5). [14]C ages obtained from the deposit underlying the delta lobes document the initiation of delta sedimentation after 3.52 cal. ka BP (Figures 3b and 5) at the northern end of the barrier, where the inlet breaches the barrier at present. Frequent and abundant overwash was also recorded in the Cies (Costas et al., 2009), where it extended to recent times due to the lower topography of the barrier. In Louro, the infilling of the lagoon by fine-grained sedimentation is observed in Transect T8. The latter alternates with aeolian and peat layers (Figure 4), suggesting several episodes of high aeolian activity followed by periods of ponds development. Environmental instability was also documented in the Traba freshwater coastal wetland record until 2.9 cal. ka BP, but was related to the migration of a diffuse drainage network due to changes in the rainfall regime (Bao et al., 2007).

Palaeo-environmental and geochemical proxies in the inner lagoon (Figure 3) indicate a change in salinity from oligohaline conditions, mainly according to the dominance of *C. placentula* in Fc10 facies, to a clear dominance of marine/brackish conditions, suggested by the presence of *O. mutabilis, C. pulchella* and *S. tabulata* in Fc8 facies. Geochemical proxies also show a strong marine influence in the Fc8 (Figure 3), and in fact the TS/TOC ratio further supports this conclusion (Figure 3). Episodes with dominance of freshwater conditions recorded at Fc10 (Figure 3) could be related to short periods

of lagoon isolation from the sea (barrier-closed). Finally, the lithogenic components such as Al and Fe are very abundant in the Fc10, suggesting a strong continental influence. All these characteristics indicate some episodes of closed-lagoon with freshwater conditions, in which muddy, organic-rich sediments dominate. Bernardez et al. (2008) observed in the NW Iberian coast a series of muddy sequences associated with high values of Fe and Al and high abundance of freshwater diatoms, for the period between 3.3 and 1.7 cal. ka BP, that were interpreted as resulting from an increase in the terrestrial inputs to the shelf due to intense rainfall and flood events. Furthermore, a similar pattern between 3 and 2 ka cal. BP was documented at the NE Iberian coast (Mojtahid et al., 2013). Towards the top, marine invasions are more evident by the distribution of the facies associations and the proxies studied in the inner lagoon. Fc8 facies shows abundant sand inputs derived from the barrier and transported towards the lagoon by the wind. Diatoms in these sand units are not only of marine/brackish affinity, as indicated above, but show a high degree of fragmentation, probably indicating a high-energy environment associated with the overwash activity on the system. In fact, in the record close to the barrier, the marine inputs are apparent by overwash events and delta formation (Figure 5), indicating a very leaky barrier and frequent breaching events. These high-energy events lead to inlet breaching and the activation of the storm corridors, which manifest closer to the present barrier position. At this time, sand can be redistributed into the lagoon by the free circulation of tidal currents when the inlet is open.

Phase 4: 1.5 cal. ka BP to present (AD 450 to present): Barrier progradation. Phase 4 is characterized by stabilization and aggradation/progradation of the barrier and episodes of reduced marine influence in the lagoon, marked by fine-grained sedimentation in the back-barrier area (Figures 4 and 5) alternating with periods of marine inflow. Bao et al. (2007) document a more stable situation for the last 2.9 cal. ka BP in Traba coastal-lake and a prevalence of freshwater conditions in the lagoon, with scarce episodes of some degree of salinity. In Louro lagoon, coarser-grained sediments confined to the north of the barrier (Transect T4, Figure 4) are interpreted as the last washover fans recorded in the area yielding an OSL age of 0.18 ka which coincides with an increase in storm intensities in the Galician coast linked to a reinforcement of the Eastern Atlantic pattern (Munoz Sobrino et al., 2014). Diatom content in Fc8 and Fc9 facies reflects some marine influence in the inner lagoon. Although the lagoon shows alternating periods of brackish and freshwaters, well-oxygenated conditions always prevailed. The upper part of the record in the inner lagoon (Figure 4) corresponds to the subsurficial zone and shows low contents in both organic and inorganic carbon, despite having plant remains and rooting. General development indicates retreat of the sand units in the inner lagoon towards the barrier and aggradation in the lagoon with muddier deposits, which is characteristic of this phase. In recent times, the development of peripheral marshes covering older washover and the flood-tidal delta deposits indicates some degree of shrinking of the lagoon area. Indeed, this appears to be a general trend observed in Traba and Cies during the last millennia (Bao et al., 2007; Costas et al., 2009). The recent decadal evolution (from AD 1970) of the barrier based on aerial photograph interpretations (Gonzalez-Villanueva, 2013) corroborates the trend observed within this fourth phase, with a reduction in the dynamism of the inlet area regulated by the water level in the lagoon and storm surges. This recent trend is also documented in Traba coastal system in relation to changes in atmospheric circulation patterns (Gonzalez-Villanueva et al., 2013). This interpretation is also supported by the dominance of brackish/freshwater to freshwater diatoms in Fc9 facies and by the deposition of muddy sediments.

External factors affecting barrier evolution: Sea-level, sediment supply, human influence and climate change

Sea-level. A decrease in the sea-level rise rate during the Holocene was mainly responsible for the onset of barrier–lagoon systems in the Atlantic coast (Alonso et al., 2003; Cearreta et al., 2003; Pages and Alonso, 2006). To study the repercussions of sealevel rise in the study area, we have included the elevation of dated deposits of known sedimentary environments along with the available sea-level curves for the interest area (Figure 6), as proposed by Alonso and Pages (2010) and Leorri et al., (2012a, 2012b). The anchoring of the barrier was set circa 8–7 cal. ka BP, following sea-level deceleration. This is indicated by the oldest samples dated in Louro lagoon when the MSL was 7–5 m below its present position. These deposits correspond to peripheral saltmarsh deposits (Figure 4) located 3–4 m below present MSL. Nowadays, these peripheral saltmarsh deposits corresponding to the ancient similar ones are located 1–1.5 m above the present MSL (2 m, AMSL). After the barrier establishment, a deceleration of sea-level rise was documented in the curves for the study area. The late evolution of the Louro barrier–lagoon system has been marked by phases of destabilization and stabilization of the sand barrier. In fact, a relative sea-level rise could be invoked as a trigger for the destabilization of the coastal barrier circa 3 cal. ka BP. However, available sea-level curves for the region (Figure 6) do not support this hypothesis (Alonso and Pages, 2010; Leorri et al., 2012a, 2012b). The existence of overwash deposits, during periods of stable sea-level, suggests that other factors (see further below) should be invoked to explain Louro barrier–lagoon evolution.

Sediment sources and budgets. Another important external factor to consider is the sediment supply. The sediment source of the first phase (i.e. barrier onset) was related to the Holocene transgression. Arribas et al. (2010) suggested that rapid sea-level rise might have provoked local erosion along the rugged Galician coast providing new sediment that remains trapped within the embayments. At present, the fluvial sediment supply as bedload is negligible, and considering the size of the river catchments and the discharges, we can assume the same pattern for the late Holocene. The Louro barrier–lagoon system is a closed system with reduced longshore currents (Almecija et al., 2008). The grain size results of the samples collected from the present-day beach and dune surface (Almecija et al., 2008) and the subsurface of the barrier show that the upper sandy units from the lagoon share a similar provenance with the present beach and dune areas. Mixed with the predominant siliciclastic grains, there is a variable amount of carbonate grains of biogenic origin, which are incorporated to the coastal systems during storms from the adjacent subtidal areas and rocky cliffs.

We hypothesize a positive sediment budget during the highstand provoking the anchoring of sand barriers and allowing the development of wide barriers. Strong onshore winds may have contributed to the formation of a large foredune and to the inland transport of sand (Phase 2, Figure 5). After this initial phase, the external sediment supply is restricted. Following the morphological continuum of Psuty (2008), once the sediment budget becomes negative, the foredune initiates its dismantling with the occurrence of blowouts that may contribute to the formation of transgressive dunes and, ultimately, with the occurrence of washovers. This situation facilitates marine inundation, as was documented in Louro barrier–lagoon (Phase 3, Figure 5), without the need of a rise in sea-level, in agreement with the available regional sealevel curves (Alonso and Pages, 2010, Leorri et al., 2012a, 2012b). In addition, an inland transport of sand would explain the observed lagoonal infill. On the other hand, the most likely sourcefor the fine-grained sedimentation in
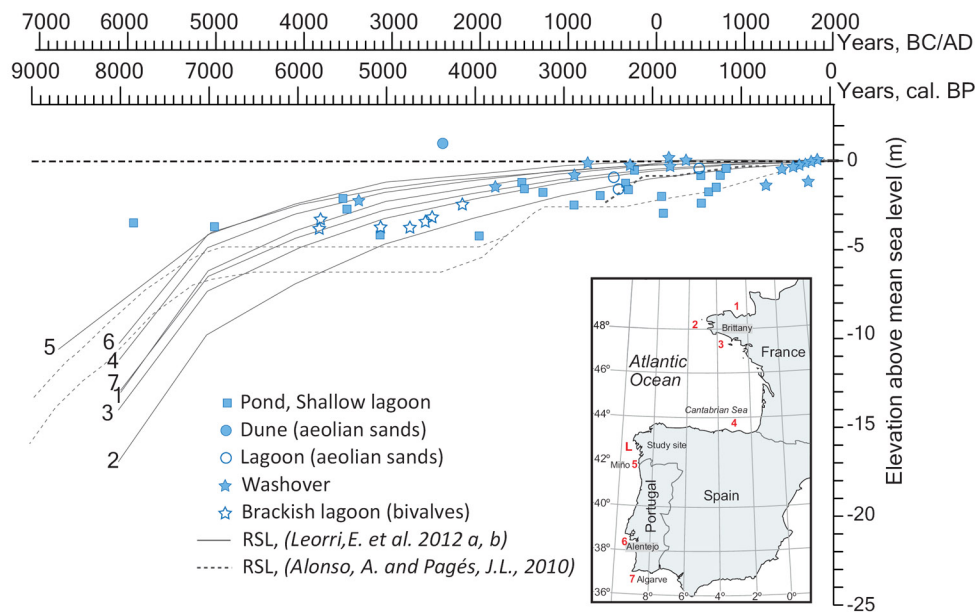
Figure 6. Sea-level change: the dashed grey line represents the relative sea-level curve in the NW Iberian Peninsula for the last 9 cal. ka BP from Alonso and Pagés (2010). 1, 2, 3, 4 and 6 grey lines correspond to relative sea-level curves along the Atlantic coast in SW Europe (Leorri et al., 2012a), and 5 grey line corresponds to relative sea-level curve in the Minho estuary (Leorri et al., 2012b). 1–6 positions are indicated in the map; letter L indicates the position of Louro coastal system. Geometric symbols represent age data (14C and OSL). All heights refer to the Alicante Mean Sea-Level – Spanish Datum System (AMSL).

the lagoon is continental input during heavy rains, both by the small channels entering the lagoon and by runoff, as indicated by the geochemical imprint of the studied sediments.

In summary, during the late Holocene, the sediment source and budget in this coastal system are the system itself. The sediment is transferred between different compartments of the system, which served as temporary 'sediment-storages' for each moment depending on the dominant external forcing factor.

Human influence. Human-derived activities directly affecting coastal systems or catchments (changes in land use, construction of urban areas, roads, etc.) may lead to increased erosion and rapid infilling of water basins, ruining the functionality of wetlands (Freitas et al., 2002; Zedler, 2004). There is a wide consensus regarding the advanced degree of infill that most of the Galician littoral lagoons show. Recent works point to non-natural processes controlling this tendency and blaming the increased sedimentation rates to the human activities, which are apparent in the last 500–600 years and become obvious for the last decades (Bao et al., 2007; Bruschi et al., 2013; Leorri et al., 2014; Mendez et al., 2011; Munoz Sobrino et al., 2014; Perez-Arlucea et al., 2005; Santos et al., 2001).

Unlike most of the examples found in the literature, Louro barrier–lagoon does not show clear signals of anthropogenic infilling. In this case, the infilling of the lagoon results from the landward migration of wind-blown deposits without clear signals of human impact over the rate of lagoon infilling. On one hand, the sediment input by tidal flooding to the lagoon is seasonal and sporadic and insufficient to explain the recent sedimentation. On the other hand, the physical characteristics of the watershed (small and steep) and the absence of a permanent river drainage network minimize the terrestrial inputs, restricting these during heavy rainfall, associated with storm events. These characteristics most likely minimize large variations in sediment source. The behaviour observed in Louro barrier–lagoon therefore differs from that of other systems in north Iberia, in which the terrestrial input due to human interventions enhanced the infill of coastal areas (Bruschi et al., 2013). Moreover, the value of sedimentation rates for the last 1000 years is the lowest in its

full history, whereas the oldest highest values are related to storm events and the instability of the barrier (Figure 3). Additionally, the concentration of metals does not show contamination in the sediments. In fact, the lower density of human population in this coastal area since historic times could explain the lower anthropogenic pressure over the system and the different behaviour observed in relation to other systems in NW Iberia. However, total P concentration is higher in the uppermost layer with respect to the lower sandy layers, indicating some degree of eutrophication. The lack of any significant human impact imprint in the infilling of Louro barrier– lagoon is, nevertheless, related to its geographic context and the low population in the study area.

Climate change. Climate change is a potential forcing factor of coastal change and barrier development. Here, the impact of climate oscillations may translate on enhanced energy reaching the coast through waves and winds. Once the barrier is attached to the coast, the subsequent evolution of the Louro system was controlled by the combination of sediment supply and onshore winds, particularly by south-westerly winds, which characterize storm conditions in the study area. These storms in Louro barrier– lagoon provoke high storm surges due to the combined effect of the atmospheric pressure and the winds, which in this area approach perpendicular to the coast (Perez-Arlucea et al., 2011). Storm surges could be responsible for temporal instabilities in the beach and/or dune, promoting the breaching of the barrier and the development of overwash deposits (Buynevich et al., 2004; Donnelly et al., 2004; Dougherty et al., 2004; Jelgersma et al., 1995; Roep et al., 1998; Ruiz et al., 2005). The latter could in turn provide information about palaeo-storm occurrence in the NW Galician coast.

Storm-related deposits dated through OSL (washover and inland dunes) are synchronous with the occurrence of other indicators pointing to enhanced storminess during the Holocene along Western Europe and Iceland (Jackson et al., 2005; Sabatier et al., 2012; Sorrel et al., 2012). In particular, they are coincident with the periods of storminess proposed by Sorrel et al. (2012), which were the result of a stacked chronology of nine independently dated records, reduc-

ing the potential influence of local environmental variability on the shared signal. Storm events along NW Europe seem to be in phase with the Holocene cooling events documented by Bond et al. (1997). During these storminess periods, a stronger meridional temperature gradient across the North Atlantic and a southward position of the westerlies has been previously suggested (Bakke et al., 2008; Magny et al., 2003). This southward position of the storm tracks implies a major impact of storms over the study area. In fact, at NW Iberia the storm periods are associated with enhanced westerly winds. This suggests that the storms affecting the study site are controlled by the regional climate of the North Atlantic. Thus, we can affirm that the analysed sedimentary record reflects regional climate signals.

Conclusion

The Holocene evolution of rocky-bounded coastal systems in NW Iberia started with the formation of freshwater peat layers associated with coastal marginal environments in the early Holocene evolving to coastal lagoon sedimentation in the middle Holocene. The main difference among these geologic controlled systems is the timing of the marine flooding, which ultimately depends on the relation between the elevation of the basin and the position of the relative MSL. When the system is located over a lower topography, as is the case of Louro, explored through this work, the MSL influenced the early evolutionary stages of the system. However, if the basement is located at a higher elevation (Cies and Traba), marine conditions will only affect sedimentation during later stages of evolution. Thus, the age of basin inundation for the coastal wetlands in NW Iberia ranged from 8 to 4 ka BP, implicating significant evolution differences among those being studied. Once marine inundation occurs, all systems evolved similarly, showing a phase of landward barrier migration and aeolian sedimentation towards the back-barrier (i.e. retrogradation). This phase extends from the onset of the marine flooding (8–4 ka BP) to circa 3.5 ka BP. The final barrier configuration (e.g. width, elevation) is determined by local factors (e.g. sediment supply) while barrier stability is controlled by regional factors (e.g. climate variability through changes in storminess).

Pervasive high-energy events, as deduced by the occurrence of several stacked washover deposits and the diatom and geochemical records in the study area, may have favoured barrier degradation in this setting of relative sea-level stability and low sediment supply. Due to its SW orientation, these high-energy events are a consequence of the Westerlies related to the cold periods of midto late Holocene. In fact, enhanced storminess conditions present a similar timing than others observed in coastal records of northern Europe and seem to be in phase with the cold Holocene climate events. This observation suggests that our sedimentary record reflects regional climate signals and represents a useful climate change indicator at a regional scale.

The absence of a significant human imprint in the sedimentary record and sediment composition suggests a quasi-non-disturbed recent evolution of this fairly well-preserved coastal system, compared with similar coastal wetlands in the region subject to accelerated infilling.

With this work, we corroborate the limitation of these sedimentary systems located in coastal embayment as sea-level indicators to reconstruct regional sea-level curves due to the important role of the basement height in the early stages of its evolution. However, the storm-related deposits are feasible indicators of the regional palaeo-storm activity.

References

Adamiec G and Aitken M (1998) Dose-rate conversion factors: Update. *Ancient TL* 16: 37–50.

Aitken J (1998) *Introduction to Optical Dating: The Dating of Quaternary Sediments by the Use of Photon-stimulated Luminescence*. Oxford: Clarendon Press.

Almecija C, Alejo I and Perez-Arlucea M (2008) Morfodinamica e hidrodinamica de una playa expuesta: ejemplo de la playa de Louro (Muros, NW Peninsula Iberica). *Geotemas* 10: 488–490.

Almecija C, Villacieros-Robineau N, Alejo I et al. (2009) Morphodynamic conceptual model of an exposed beach: The case of Louro Beach (Galicia, NW, Iberia). *Journal of Coastal Research SI* 56: 1711–1715.

Alonso A and Pages JL (2010) Evolucion del nivel del mar durante el Holoceno en el noroeste de la Peninsula Iberica. *Revista de la Sociedad Geologica de Espana* 23: 11.

Alonso A, Pages JL, Lopez Garcia MJ et al. (2003) Cronoestratigrafia de la transgresion holocena en el Golfo Artabro (La Coruna, NO de Espana). In: Flor G (ed.) *Actas de la XI Reunion Nacional del Cuaternario*. Oviedo: Universidad de Cantabria, pp. 33–38.

Arribas J, Alonso A, Pages JL et al. (2010) Holocene transgression recorded by sand composition in the mesotidal Galician coastline (NW Spain). *The Holocene* 20: 375–393.

Bakke J, Lie O, Dahl SO et al. (2008) Strength and spatial patterns of the Holocene wintertime westerlies in the NE Atlantic region. *Global and Planetary Change* 60: 28–41.

Bao R, Alonso A, Delgado C et al. (2007) Identification of the main driving mechanisms in the evolution of a small coastal wetland (Traba, Galicia, NW Spain) since its origin 5700 cal yr BP. *Palaeogeography, Palaeoclimatolology, Palaeoecology* 247: 296–312.

Bao R, Freitas MC and Andrade C (1999) Separating eustatic from local environmental effects: A late-Holocene record of coastal change in Albufeira Lagoon, Portugal. *The Holocene* 9: 341–352.

Bernardez P, Gonzalez-Alvarez R, Frances G et al. (2008) Late Holocene history of the rainfall in the NW Iberian peninsula–Evidence from a marine record. *Journal of Marine Systems* 72: 366–382.

Bjorck S and Wohlfarth B (2001) 14C chronostratigraphic techniques in paleolimnology. In: Last WM and Smol JP (eds) *Tracking Environmental Changes Using Lake Sediments*. Dordrecht: Kluwer, pp. 205–245.

Blanco-Chao R, Costa Casais M, Martinez Cortizas A et al.(2002) Holocene evolution on Galician coast (NW Spain): An example of paraglacial dynamics. *Quaternary International* 93–94: 149–159.

Blott SJ and Pye K (2001) GRADISTAT: A grain size distribution and statistics package for the analysis of unconsolidated sediments. *Earth Surface Processes and Landforms* 26:1237–1248.

Bond G, Showers W, Cheseby M et al. (1997) A pervasive millennial-scale cycle in North Atlantic Holocene and glacial climates. *Science* 278: 1257–1266.

Bruschi VM, Bonachea J, Remondo J et al. (2013) Analysis of geomorphic systems' response to natural and human drivers in northern Spain: Implications for global geomorphic change. *Geomorphology* 196: 267–279.

Buynevich IV, FitzGerald DM and van Heteren S (2004) Sedimentary records of intense storms in Holocene barrier sequences, Maine, USA. *Marine Geology* 210: 135–148.

Cabral MC, Freitas MC, Andrade C et al. (2006) Coastal evolution and Holocene ostracods in Melides lagoon (SW Portugal). *Marine Micropaleontology* 60: 181–204.

Cambardella CA, Gajda AM, Doran JW et al. (2000) Estimation of particulate and total organic matter by weight losson-ignition. In: Kimble JM, Follett RF and Stewart BA (eds) *Assessment Methods for Soil Carbon*. Boca Raton, FL: Taylor & Francis, pp. 349–359. Cameron TDJ, Stoker MS and Long D (1987) The history of Quaternary sedimentation in the UK sector of the North Sea Basin. *Journal of the Geological Society* 144: 43–58.

Casquet C and Fernandez de la Cruz MN (1981) Hoja geologica No119 (Noya). In: *Mapa geologico E.:1:50.0000* (Segunda serie I.G.M.E.). Madrid: Instituto Geologico y Minero de Espana.

Cearreta A, Cachao M, Cabral MC et al. (2003) Lateglacial and Holocene environmental changes in Portuguese coastal lagoons 2: Microfossil multiproxy reconstruction of the Santo Andre coastal area. *The Holocene* 13: 447–458.

Clark PU, Dyke AS, Shakun JD et al. (2009) The Last Glacial Maximum. *Science* 325: 710–714.

Clark PU, McCabe AM, Mix AC et al. (2004) Rapid rise of sea level 19,000 years ago and its global implications. *Science* 304: 1141–1144.

Clemmensen LB, Andreasen F, Nielsen ST et al. (1996) The late Holocene coastal dunefield at Vejers, Denmark: Characteristics, sand budget and depositional dynamics. *Geomorphology* 17: 79–98.

Clemmensen LB, Murray A, Heinemeier J et al. (2009) The evolution of Holocene coastal dunefields, Jutland, Denmark: A record of climate change over the past 5000 years. *Geomorphology* 105: 303–313.

Cobelo-Garcia A, Bernardez P, Leira M et al. (2012) Temporal and diel cycling of nutrients in a barrier–lagoon complex: Implications for phytoplankton abundance and composition. *Estuarine, Coastal and Shelf Science* 110: 69–76.

Costas S, Munoz-Sobrino C, Alejo I et al. (2009) Holocene evolution of a rock-bounded barrier-lagoon system, Cies Islands, northwest Iberia. *Earth Surface Processes and Landforms* 34: 1575–1586.

Davies JL (1964) A morphogenetic approach to world shorelines. *Zeitschrift fur Geomorphology* 8: 127–142.

Dellwig O, Watermann F, Brumsack HJ et al. (1999) High-resolution reconstruction of a Holocene coastal sequence (NW Germany) using inorganic geochemical data and diatom inventories. *Estuarine, Coastal and Shelf Science* 48: 617–633.

Demarest JM and Leatherman SP (1985) Mainland influence on coastal transgression: Delmarva Peninsula. *Marine Geology* 63: 19–33.

Devoy RJN, Delaney C, Carter RWG et al. (1996) Coastal stratigraphies as indicators of environmental changes upon European Atlantic Coasts in the Late Holocene. *Journal of Coastal Research* 12: 564–588.

Donnelly JP, Butler J, Roll S et al. (2004) A backbarrier overwash record of intense storms from Brigantine, New Jersey. *Marine Geology* 210: 107–121.

Dougherty AJ, FitzGerald DM and Buynevich IV (2004) Evidence for storm-dominated early progradation of Castle Neck barrier, Massachusetts, USA. *Marine Geology* 210: 123–134.

European Environmental Agency (EEA) (2006) *The Changing Faces of Europe's Coastal Areas*. Copenhagen: EEA.

Feal-Perez A, Blanco-Chao R, Ferro-Vazquez C et al. (2014) Late-Holocene storm imprint in a coastal sedimentary sequence (Northwest Iberian coast). *The Holocene* 24: 477–488.

Fomento MD (1991) Atlas del Clima Maritimo en el Litoral. In: Puertos del Estado (ed.) *ROM*. Madrid: Ministerio de Fomento, 55 pp.

Fraga P (2013) *Dinamica espacio-temporal de la composicion y geoquimica de las aguas y sedimentos de la laguna de Louro*. Santiago de Compostela: Universidade de Santiago de Compostela, 75 pp.

Freitas MC, Andrade C and Cruces A (2002) The geological record of environmental changes in southwestern Portuguese coastal lagoons since the Lateglacial. *Quaternay International* 93–94: 161–170.

Freitas MC, Andrade C, Rocha F et al. (2003) Lateglacial and Holocene environmental changes in Portuguese coastal lagoons 1: The sedimentological and geochemical records of the Santo Andre coastal area. *The Holocene* 13: 433–446.

Gee GW and Bauder JW (1986) Particle-size analysis. In: Klute EA (ed.) *Methods of Soil Analysis: Part 1 – Physical and Mineralogical Methods*. Madison, WI: American Society of Agronomy and Soil Science Society of America, pp. 383–412.

Gonzalez-Villanueva R (2013) *Origin, evolution and processes controlling Holocene barrier-lagoon systems (NW Spain)*. PhD Thesis, Geociencias Marinas y Ordenacion del Territorio, Universidad de Vigo, 199 pp.

Gonzalez-Villanueva R, Costas S, Perez-Arlucea M et al. (2011) Evolution of the southern dune sector of Corrubedo complex. *Geogaceta* 50: 4.

Gonzalez-Villanueva R, Costas S, Perez-Arlucea M et al. (2013) Impact of atmospheric circulation patterns on coastal dune dynamics, NW Spain. *Geomorphology* 185: 96–109.

Hou G, Lai Z, Sun Y et al. (2012) Luminescence and radiocarbon chronologies for the Xindian Culture site of Lamafeng in the Guanting Basin on the NE edge of the Tibetan Plateau. *Quaternary Geochronology* 10: 394–398.

Jackson MG, Oskarsson N, Tronnes RG et al. (2005) Holocene loess deposition in Iceland: Evidence for millennial-scale atmosphere-ocean coupling in the North Atlantic. *Geology* 33: 509–512.

Jelgersma S, Stive MJF and van der Valk L (1995) Holocene storm surge signatures in the coastal dunes of the western Netherlands. *Marine Geology* 125: 95–110.

Leorri E, Cearreta A and Milne G (2012a) Field observations and modelling of Holocene sea-level changes in the southern Bay of Biscay: Implication for understanding current rates of relative sea-level change and vertical land motion along the Atlantic coast of SW Europe. *Quaternary Science Reviews* 42: 59–73.

Leorri E, Fatela F, Drago T et al. (2012b) Lateglacial and Holocene coastal evolution in the Minho estuary (N Portugal): Implications for understanding sea-level changes in Atlantic Iberia. *The Holocene* 23: 353–363.

Leorri E, Mitra S, Irabien MJ et al. (2014) A 700 year record of combustion-derived pollution in northern Spain: Tools to identify the Holocene/Anthropocene transition in coastal environments. *Science of the Total Environment* 470–471: 240–247.

Macias Vazquez F and Calvo de Anta R (2009) *Niveles genericos de referencia de metales pesados y otros elementos traza en suelos de Galicia*. Conselleria de Medio Ambiente e Desenvolvemento Sostible (Xunta de Galicia). Available at: http://solos.medioambiente.xunta.es/solos/documents/librongr.pdf.

Magny M, Begeot C, Guiot J et al. (2003) Contrasting patterns of hydrological changes in Europe in response to Holocene climate cooling phases. *Quaternary Science Reviews* 22:1589–1596.

Martinez Cortizas A and Perez Alberti A (1999) *Atlas Climatico de Galicia*. A Coruna: Xunta de Galicia.

Masselink G and Short AD (1993) The effect of tide range on beach morphodynamics and morphology: A Conceptual Beach Model. *Journal of Coastal Research* 9: 785–800.

Mendez G, Perez-Arlucea M, Gonzalez-Villanueva R et al.(2011) Anthropogenic influence on the Holocene sedimentation process along the Atlantic coast of Galicia (NW Iberian Peninsula). *Journal of Coastal Research* SI 64: 4.

Mendez G, Perez-Arlucea M, Stouthammer E et al. (2003) The TESS-1 suction corer: A new device to extract wet, uncompacted sediments. *Journal of Sedimentary Research* 73: 1078–1081.

Merian E (1991) *Metals and Their Compounds in the Environment*. New York: Wiley-VCH.

Meyers PA and Lallier-verges E (1999) Lacustrine sedimentary organic matter records of late quaternary paleoclimates. *Journal of Paleolimnology* 21: 345–372.

Mojtahid M, Jorissen FJ, Garcia J et al. (2013) High resolution Holocene record in the southeastern Bay of Biscay: Global versus regional climate signals. *Palaeogeography, Palaeoclimatology, Palaeoecology* 377: 28–44.

Munoz Sobrino C, Garcia-Moreiras I, Castro Y et al. (2014) Climate and anthropogenic factors influencing an estuarine ecosystem from NW Iberia: New high resolution multiproxy analyses from San Simon Bay (Ria de Vigo). *Quaternary Science Reviews* 93: 11–33.

Murray AS and Clemmensen LB (2001) Luminescence dating of Holocene aeolian sand movement, Thy, Denmark. *Quaternary Science Reviews* 20: 751–754.

Nichols MM (1989) Sediment accumulation rates and relative sea-level rise in lagoons. *Marine Geology* 88: 201–219.

Niedoroda AW, Swift DJP, Figueiredo AG et al. (1985) Barrier island evolution, middle Atlantic shelf, U.S.A. Part II: Evidence from the shelf floor. *Marine Geology* 63: 363–396.

Otvos EG (1981) Barrier Island formation through nearshore aggradation – Stratigraphic and field evidence. *Marine Geology* 43: 195–243.

Pages JL and Alonso A (2006) Evolucion Holocena del paisaje litoral del Noroeste de la Peninsula Iberica. In: *Geomorfologia y territorio: actas de la IX Reunion Nacional de Geomorfologia* (ed A Perez Alberti and J Lopez Bedoya), Santiago de Compostela, 13–15 de septiembre de 2006. Santiago de Compostela: Universidade de Santiago de Compostela, pp. 443–456.

Perez-Arlucea M, Almecija C, Gonzalez-Villanueva R et al.(2011) Water dynamics in a barrier-lagoon system: controlling factors. *Journal of Coastal Research* SI 64: 15–19.

Perez-Arlucea M, Mendez G, Clemente F et al. (2005) Hydrology, sediment yield, erosion and sedimentation rates in the estuarine environment of the Ria de Vigo, Galicia, Spain. *Journal of Marine Systems* 54: 209–226.

Prescott JR and Hutton JT (1994) Cosmic ray contributions to dose rates for luminescence and ESR dating: Large depths and long-term time variations. *Radiation Measurements* 23: 497–500.

Psuty N (2008) The coastal foredune: A morphological basis for regional coastal dune development coastal dunes. In: Martinez M and Psuty N (eds) *Coastal Dunes Ecology and Conservation*. Berlin, Heidelberg: Springer, pp. 11–27.

Psuty NP, Eugenia M and Moreira SA (2000) Holocene sedimentation and sea level rise in the Sado Estuary, Portugal. *Journal of Coastal Research* 16: 125–138.

Rampino MR and Sanders JE (1981) Evolution of the barrier islands of southern Long Island, New York. *Sedimentology* 28: 37–47.

Reimer PJ, Baillie MGL, Bard E et al. (2009) IntCal09 and Marine09 radiocarbon age calibration curves, 0–50,000 years cal BP. Available at: https://journals.uair.arizona.edu/index.php/radiocarbon/article/view/3569.

Renberg I (1990) A procedure for preparing large sets of diatom slides from sediment cores. *Journal of Paleolimnology* 4: 87–90.

Roep TB, Dabrio CJ, Fortuin AR et al. (1998) Late highstand patterns of shifting and stepping coastal barriers and washover-fans (late Messinian, Sorbas Basin, SE Spain). *Sedimentary Geology* 116: 27–56.

Ruiz F, Rodriguez-Ramirez A, Caceres LM et al. (2005) Evidence of high-energy events in the geological record: Mid-holocene evolution of the southwestern Donana National Park (SW Spain). *Palaeogeography, Palaeoclimatology, Palaeoecology* 229: 212–229.

Sabatier P, Dezileau L, Colin C et al. (2012) 7000 years of paleostorm activity in the NW Mediterranean Sea in response to Holocene climate events. *Quaternary Research* 7: 1–11.

Sancetta C (1979) Use of semiquantitative microfossil data for paleoceanography. *Geology* 7: 88–92.

Santos L, Bao R and Sanchez Goni MF (2001) Pollen record of the last 500 years from the Doninos coastal lagoon (NW Iberian Peninsula): Changes in pollinic catchment size *versus* paleoecological interpretation. *Journal of Coastal Research* 17: 705–713.

Sorrel P, Debret M, Billeaud I et al. (2012) Persistent non-solar forcing of Holocene storm dynamics in coastal sedimentary archives. *Nature Geoscience* 5: 892–896.

Stuiver M, Reimer PJ and Reimer RW (2005) CALIB 7.0.2 (program and documentation). Available at: http://calib.qub.ac.uk/calib/download/.

Trobajo R and Sullivan MJ (2010) Applied diatom studies in estuaries and shallow coastal sediments. In: Smol JP and Stoermer EF (eds) *The Diatoms: Applications for the Environmental and Earth Sciences*. Cambridge: Cambridge University Press, pp. 309–323.

Vos P and Wolf H (1993) Diatoms as a tool for reconstructing sedimentary environments in coastal wetlands; methodological aspects. *Hydrobiologia* 269–270: 285–296.

Zedler JB (2004) Compensating for wetland losses in the United States. *Ibis* 146: 92–100.